Title	Precise Determination of Crystallite Size of Ultra-drawn Ultra-high Molecular Weight Polyethylene (Commemoration Issue Dedicated to Professor Hisashi Odani On the Occasion of His Retirement)
Author(s)	Kawaguchi, Akiyoshi; Murakami, Syozo; Tsuji, Masaki; Ohta, Toshihiko
Citation	Bulletin of the Institute for Chemical Research, Kyoto University (1992), 70(2): 188-197
Issue Date	1992-09-30
URL	http://hdl.handle.net/2433/77444
Right	
Type	Departmental Bulletin Paper
Textversion	publisher

Precise Determination of Crystallite Size of Ultra-drawn Ultra-high Molecular Weight Polyethylene

Akiyoshi Kawaguchi*, Syozo Murakami*, Masaki Tsuji* and Toshihiko Ohta**

A thin "plate-like sample" of ultra-drawn ultra-high molecular weight polyethylene (UD-UHMWPE) with the chain axis normal to it was specially prepared: a UD-UHMWPE rod 1 mm in diameter was sectioned perpendicularly to the rod axis into discs of a thickness of 0.3 mm and they were arranged flat-on on a glass plate. The 002 diffraction profile of the sample was measured by the step scanning method in the reflection mode. From the profile thus accurately measured, the pure diffraction profile of the sample was extracted by the deconvolution method of the iterative convolution, with referrence to the instrumental broadening obtained from the Si diffraction profile. The crystallite size as large as 91.1 nm was evaluated from the integral breadth obtained by applying the least squares curve fitting method to the pure curve, but the corresponding long period was not identified in the small angle X-ray scattering pattern.

KEYWORDS : Ultra-high molecular weight polyethylene / Wide angle X-ray diffraction / Small angle X-ray scattering / Deconvolution / Crystallite size

INTRODUCTION

Excellent mechanical properties such as high elastic modulus and high strength of ultra-drawn ultra-high molecular weight polyethylene(UD-UHMWPE) were performed by super-drawing of cast films from solution[1] or single crystal mats[2,3]. The high performance of UD-UHMWPE is largely affected by the microstructures, e.g., the crystallite size and disorder along the molecular axis and the degree of molecular orientation, which are seen in papers and monographs[4,5]. In the present paper, we will focus on how large crystallites are grown in UD-UHMWPE. The crystallite size has been measured by X-ray diffraction[4] and by dark field and high resolution electron microscopy[6,7]. Here, we tried to accurately measure the diffraction curves by employing the former method and to estimate the crystallite size through the precise analyses of the profile. The experimental procedure to obtain the accurate profiles of diffractions perpendicular to the c-axis of thin films or fibers and the mothod of profile analysis are detailed. The obtained results of crystallite size are briefly discussed in comparison with the long periods observed by small angle X-ray scattering.

---

* 河口昭義, 村上昌三, 辻　正樹 : Division of States and Structures, Laboratory of Polymer Condensed States, The Institute for Chemical Research, Kyoto University, Uji, Kyoto 611.
** 太田利彦 : The Faculty of Science of Living, Osaka City University, Sumiyoshi-ku, Osaka 586.

EXPERIMENTAL

A highly oriented PE rod of a diameter of about 1 mm was sectioned perpendicular to the rod axis into discs of a thickness of 0.3 mm. The small PE discs thus made, in which the c-axis is pependicular to the flat surface, were arranged on a glass slide surface as shown in Fig. 1a. The glass slide was set on the head of a goniometer in the reflection mode as shown in Fig. 1b. In this setting, the 002 diffraction profile of a "thin PE plate with the c-axis normal to it" was able to be measured. X-ray measurements were carried out by the step scanning method at an angular interval of 1/100 degree. The Ni-filtered CuKα radiation was used.

The small angle X-ray scattering apparatus used here consisted of pin-hole collimators set at the sepatation of 1.5 m and the sample-to-camera distance was 1.35 m.
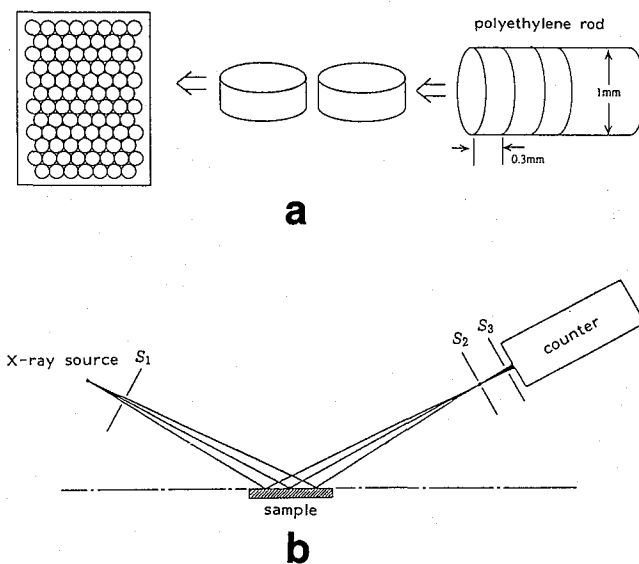

a

b

Fig. 1. (a) Method to prepare a "thin plate-like sample with chain axes normal to the surface" from a PE rod. (b) The setting of the plate on a goniometer in the reflection mode. S_1, S_2 and S_3 are the divergent, receiving and scatter slits, respectively.

Ultra-drawn ultra-high molecular weight polyethylene(UD-UHMWPE)(Hizex 240 M, $Mw=2\times10^6$ with a high modulus of 175 GPa) and highly drawn high density polyethylene (HDPE) (Sholex 6009, MI=9) were examined. The UD-UHMWPE rod was prepared by ultra-drawing of a pressed sheet made of gel-like spherulites[8]. For evaluation of the instrumental broadening, the diffraction profile of the Si powder was measured.

A. KAWAGUCHI, S. MURAKAMI, M. TSUJI and T. OHTA

LINE PROFILE ANALYSIS

In the X-ray measurement, a pure diffraction profile basing on the crystallinity of a sample is inevitably broadened by various geometrical causes of a diffractometer and by the transparency of X-rays of the sample. The broadening is mathematically expressed by the convolution of a pure diffraction profile of a sample with the weight functions expressing the experimentally unavoidable broadenings. When the pure diffraction profile and an experimental weight function are denoted as f(x) and g(x), respectively, the broadened function h(x) is described by the following integral:

$$h(x) = \int f(y)g(x-y)dy \tag{1},$$

where the variable x is here the scattering angle of 2θ and the auxiliary variable y has the same dimension as 2θ. The expression (1) is abbreviated to $f(x) * g(x)$ in which $*$ denotes the convolution operation. There are various instrumental origins producing broadening even in a well-aligned parafocusing diffractometer; the shape of focal profile of X-ray source(g_1), the use of a flat specimen(g_2), the axial divergence of incident beams(g_3), the shape of a receiving slit(g_4) and the misalignment of a goniometer(g_5). The expressions $g_j(j=1,5)$ mean the weight function for the respective broadenings. The total broadening function $g_i(x)$ as a combined effect of these broadenings is then expressed by the multiple convolution of these functions[9],

$$g_i(x) = g_1(x) * g_2(x) * g_3(x) * g_4(x) * g_5(x) \tag{2}$$

The function $g_i(x)$ is independent of the nature of sample, and hence the total broadening by above origins of 1 to 5 is here called the instrumental broadening. Another broadening is given rise to by the penetration of X-rays into the specimen with a finite absorption coefficient μ (elsewhere, the broadening is involved in the instrumental broadening). This broadening depends on the atomic constitution and shape, especially thickness, of sample, and its weight function (g_6) is expressed[10] by

$$g_6(x) = (1-u/a)\exp(-Au) \tag{3}.$$

In the equation, $u=2t\cos\theta/R$ where t is the depth from the sample surface, θ the Bragg angle and R the sample-to-receiving slit distance and $A=2\mu R/\sin\theta$. Thus, the total broadening g(x) is described below:

$$g(x) = g_i(x) * g_6(x) \tag{4}.$$

When the absorption coefficient is sufficiently large, the convolution (4) is practically approximated to $g_i(x)$. This implies that the instrumental broadening is actually realized as the diffraction profile of the materials with the large μ and large crystallite size. We can experimentally get the total instrumental broadening function $g_i(x)$ using such a crystalline specimen, without knowing each function of g_1 to g_5. It is important, however, for this

purpose to select an approriate material consisting of sufficiently large and strain-free crystallites, exhibiting the exceedingly sharp reflections in the above angular range of reflection. The 002 PE reflection profile ranging from $2\theta=72°$ to $2\theta=75°$ is interesting here. Accordingly, the crystalline Si powder with the density $\rho=2.3$ g/cm^3 was used for that purpose, having a diffraction peak of 76.375° for CuKα_1 rays and the mass absorption coefficient μ $=60.6$ cm^2/g (cf., $\mu=4.0$ cm^2/g for PE with $\rho=1.0$ g/cm^3).

An as-observed diffraction profile h(x) is expressed by the convolution (1) of a pure diffraction profile of sample f(x) with the instrumental broadening g(x). In order to measure physical parameters of crystals such as the crystallite size and lattice strain or disorder, we are faced with a big problem of extracting the profile f(x) from the profile h(x). Though the extraction can be performed by a deconvolution procedure, e.g., by the Fourier transformation[11] or the iterative method of convolution[12], it involves enormous steps of computing. Recently, as the potential of a personal computer is much improved, the deconvolution by the above methods can very easily be done with the help of it. Here, the latter convolution method is employed because of its simplicity. Actually, the deconvolution by the iterative method is conducted according to the following procedure. First, the as-observed curve h(x) is assumed to be the pure diffraction profile as the zeroth approximation $f_0(x)$. The difference is obtained by substracting the convolution $g(x) * f_0(x)$ from h(x) and added to $f_0(x)$. The resulted function $f_1(x)$ gives the first approximation to f(x):

$$f_1(x)=f_0(x)+\{h(x)-f_0(x) \cdot g(x)\}. \tag{5}$$

The second approximation function $f_2(x)$ is obtained by iterating the above process, after $f_0(x)$ is replaced with $f_1(x)$. Iterations are continued, for example, untill the difference between h(x) and $g(x) * f_n(x)$ (n: the cycle number of convolution) reaches a certain value of the same magnitude as the statistical accuracy of h(x) and g(x).

Since only one profile data of 002 reflection was available, the crystallite size is discussed on the basis of the integral breadth. The least squares curve fitting method was applied to the pure diffraction profile thus obtained, so that the integral breadth was evaluated. The following pseud-Voigt function in which the Lorentzian and Gaussian functions are combined as below was used for curve fitting[13]:

$$f(x)=(1-c)h/[1+\{(x-p)/w\}^2]+c \cdot h \cdot \exp[-\{(x-p)/w\}^2] \tag{6},$$

where p,w,h and c denote the peak position of a diffraction curve, the half-value width, the peak height and the fraction of Gaussian component, respectively.

RESULTS AND DISCUSSION

The curve A in Fig. 2 shows the 331 diffraction profile of Si powder obtained by the step scanning method. The background is ascribed mainly to scattering by air and to incoherent scattering. The background intensity is simply subtracted from the total scattering curve (see the curve B in Fig. 2), and the resulted intensity curve is divided by the total intensity summed up over the full angular range of observation:

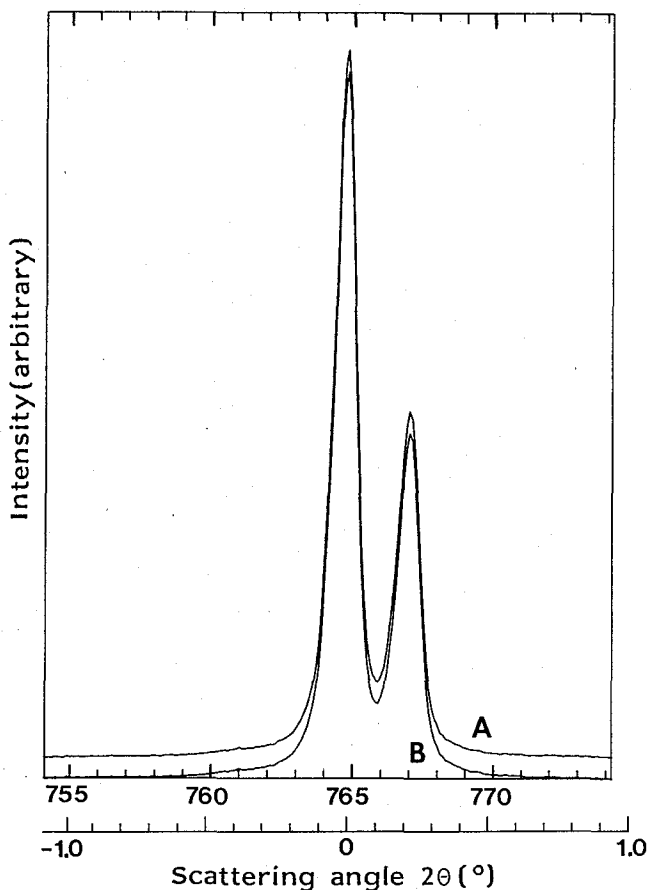A. KAWAGUCHI, S. MURAKAMI, M. TSUJI and T. OHTA

Fig. 2. Curve A is the as-measured profile of the 331 reflection of Si powder and the curve B
is one after subtraction of the background intensity.

$$\int_a^b I'(x)dx = 1 \tag{7},$$

where a and b are the lower and upper angular limits, reapectively, and $I'(x)$ the intensity
thus normalized after subtraction of background. The normalized intensity curve is
assumed to be the weight function for instrumental broadening, $g_i(x)$, where the abscissa (x-
axis) is re-defined so that the origin is allocated to the scattering angle of peak intensity.
The function is convoluted with the weight function $g_6(x)$ of PE sample with the absorption
coefficient $\mu = 4.0$ cm^2/g for CuKα_1 and the thickness of sample t=0.03 cm. The resulted
weight function after the convolution is almost unchanged from $g_i(x)$.

Figure 3 shows an as-measured profile of UHMWPE and a series of deconvoluted
curves. The as-measured profile (the curve with n=0) exhibits the double peaks due to
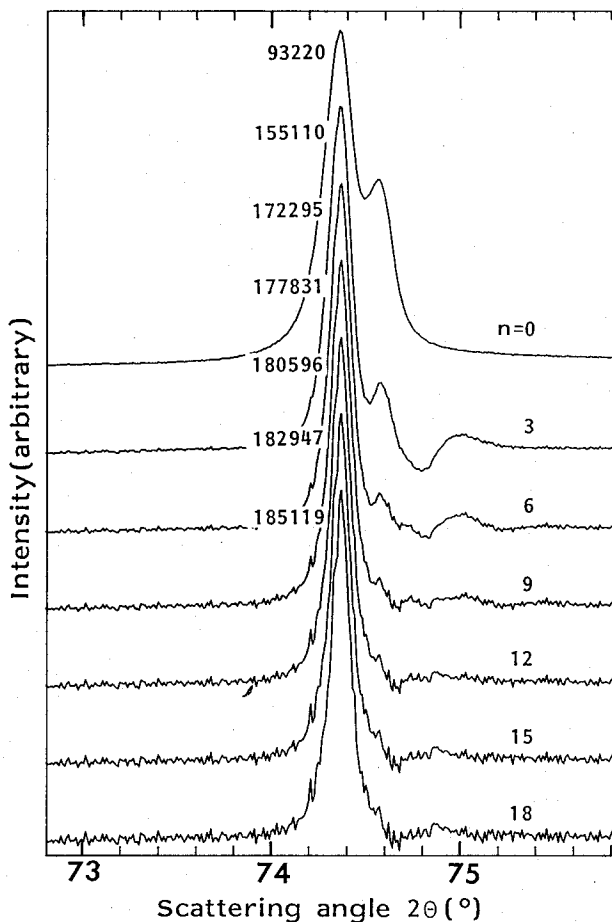the doublet of CuKα_1 and CuKα_2 radiations. It is clearly seen that the double peaks are

Fig. 3. As-mesured and deconvoluted 002 PE reflection profiles of UD-UHMWPE. n denotes the cycle number of convolution and the figures on the left side of the peaks the intensities of respective curves.
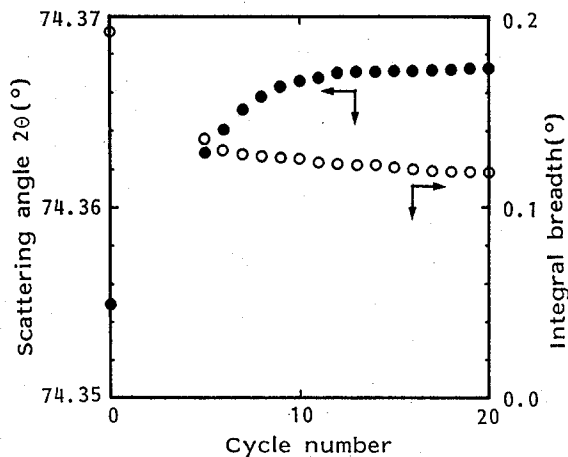
Fig. 4. Scattering angle 2θ at peak and the integral breadth as a function of the cycle number of convolution for UD-UHMWPE.

transfigured into a single peak corresponding to that by $CuK\alpha_1$ as iterations continue and that the profile becomes sharper. Since the effect of the doublet of incident X-rays on the instrumental broadening is also realized as double peaks, the transfiguration into the single peak profile indicates that the deconvoltion was successfully performed. This means that if the measurement is carried out using the perfectly monochromatized X-rays of $CuK\alpha_1$ only, the single peak is recorded. The most powerful X-ray source available in a laboratory scale is a rotating anode X-ray generator operated at a current of at highest 1 Ampere. Even by the use of this type of high-power X-ray generator, it is not practical to carry out the diffraction works using the monochromatized X-rays with $K\alpha_1$ only, because its intensity is exceedingly reduced when the monochromatization was achieved perfectly in this way.

The shift of peak position and the change of integral breadth are shown in Fig. 4 against the cycle number of iteration. A reasonable convergence is indeed achieved after ten cycles. If additional cycles are conducted, the ripples along the curve are marked and the processed curve is more and more diverse as seen in Fig. 3, especialy at the parts where the as-measured curve is divergent. So, the rippling is marked in the less-smoothed curve with a low ratio of signal to noise. It is found from Fig. 4, however, that even though the curve is more disordered, the integral breadth obtained by applying the least squares curve fitting method to it is convergent to a constant value. Besides the rippling, the slow undulation of the deconvoluted curve remains along the tail on the higher angle side. The observed g(x) function is not completely compatible with the observed PE profile h(x): for the peak positions of the 002 PE reflection and the 331 Si reflection are not the same and hence the angular separation of the 002 PE reflection due to $CuK\alpha_1$ and $CuK\alpha_2$ doublet (0.205 degree) is smaller than that of the 331 Si reflection (0.223 degree). This difference probably causes the undulation. Figures 5 and 6 shows the results obtained for drawn HDPE.

Table 1 shows crystalline data of UHMWPE and HDPE obtained by analysing the deconvoluted curves by the least squares method[13]. Crystallites as large as 91.1 nm were formed in UD-UHMWPE. Such large crystallites exceeding 100 nm and reaching 1 μm are really observed by electron microscopy of highly drawn isotactic polystyrene[15] and the UD-UHMWPE film[7]. In the table 1, the long period of HDPE measured by the small angle X-ray scattering and the crystallite size estimated by the Scherrer equation from the integral breadth[14] are compared. The line profile is broadened not only by the crystallite size but also by the lattice strain or disorder. The integral breadths obtained in the present way correspond to the value of strain-free lattice. Further, we must suspect that the lattice disorder may be introduced in the process of sample preparation of sectioning PE rods. Hence, the real crystallite size may be larger. In order to estimate both simultaneously, the line profiles of different order of reflections, i.e., the 002 and 004 reflections in PE,

Table 1

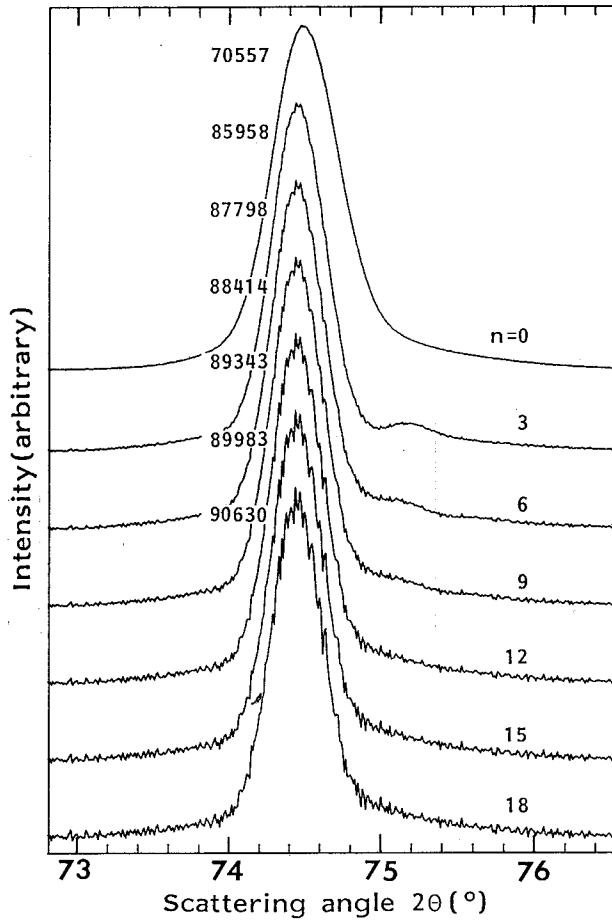|	long period (nm)	crystallite size(nm)	d(002) (nm)
HDPE	34.6	28.6	0.1274
UD-UHMWPE	—	91.1	0.1276

Fig. 5. As-measured and deconvoluted 002 PE reflection profiles of highly drawn HDPE. n denotes the cycle number of convolution and the figures on the left side of the peaks the intensities of respective curves.
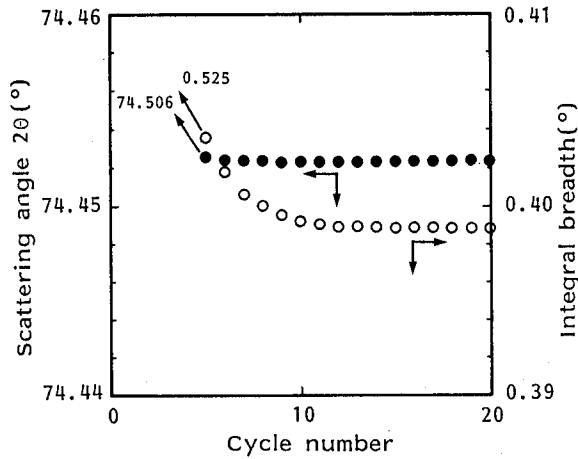

Fig. 6. Scattering angle 2θ at peak and the integral breadth as a function of cycle number of convolution for highly drawn HDPE.

must be analyzed, but as long as the CuKα X-rays is used, only the 002 reflection profile is measurable.

Figure 7 shows the small angle X-ray scattering patterns(SAXSPs) of HDPE and UHMWPE. The discrete scattering peaks are clearly seen in the meridional direction of the SAXSP of HDPE in Fig. 7a. As wellknown, the long period is larger than the crystallite size along the c-axis. The crystalline regions are stacked along the c-axis, noncrystalline regions with the lower electron density than that of crystalline region intervening between them. Noncrystalline regions are found to be about 6 nm thick. In UHMWPE, the crystallites along the c-axis are also finite with as large dimension as 91.1 nm. This implies that crystallites are bounded by noncrystalline regions at both ends. The dumbell-like scattering meridionally extended is observed in the SAXSP of Fig. 7b. Since such scattering is not seen in Fig. 7a, which is taken for a much longer exposure time than Fig. 7b, there is no doubt that the scattering originated from the UD-UHMWPE sample. The resolution of the present small angle X-ray scattering apparatus is as high as 100 nm. However, the long period, if exists, compares to it, and the scattering itself is too broad to identify as a discrete peak. Thus, from the view point of the resolution limit, we cannot decide from Fig.
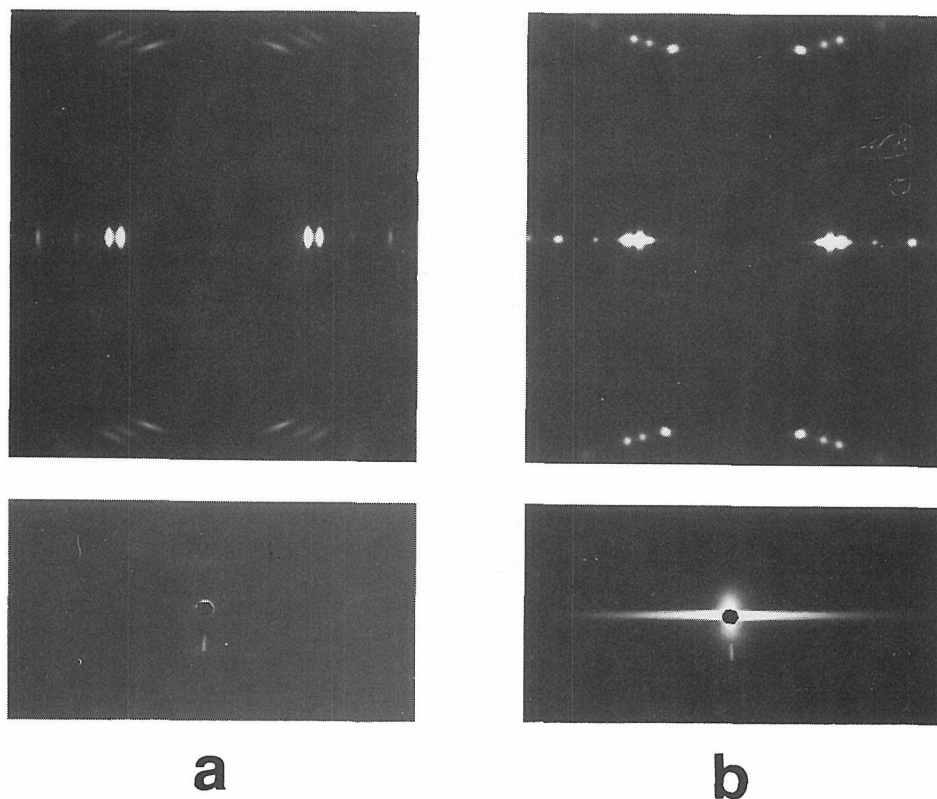

a   b

Fig. 7. Wide angle(upper) and small angle(lower) X-ray scattering patterns of (a)HDPE and (b)UD-UHMWPE.

7b that the long period exists and that the crystalline and noncrystalline regions are stacked alternatively along the c-axis. Whether or not the long period is observed depends on the stacking order of crystallites and the distribution of their size. The relation between the crystallite size and the dumbell-like scattering at small angles will be elucidated.

REFERENCES

1) P. Smith, P.L. Lemstra, J.P.L. Pijpers and A.M. Kiel, *Colloid and Polym. Sci.*, **254**, 1070 (1981).
2) T. Kanamoto, A. Tsuruta, K. Tanaka, M. Takeda and R.S. Porter, *Polymer J.*, **15**, 327 (1983).
3) K. Furuta, T. Yokokawa, and K. Miyasaka, *J. Polymer Sci., Polymer Phys. Ed.*, **22**, 133 (1984).
4) K. Nakamae, T. Nishio and H. Ohkubo, *J. Macromol. Sci.-Phys.*, **B30**, 1 (1991).
5) P.J. Lemstra, R. Krishbaum, T. Ohta and H. Yamada, "Development in Oriented Polymers-2" ed. by I.M. Ward, Elsevier Appl. Sci. Publ., London and New York, 1987.
6) H.D. Chanzy, P. Smith, J.-F. Revol and R.St. John Manley, *Polymer Comm.*, **28**, 133 (1987).
7) J.M. Brady and E.L. Thomas, *Polymer*, **30**, 1615 (1987).
8) T. Ohta, F. Okada, M. Hayashi and M. Mihoichi, *Polymer*, **30**, 2171 (1989).
9) "X-ray Diffraction Procedure", 2nd Ed., by H.P. Klug and L.E. Alexander, John Wiley & Sons, New York, 1974.
10) C. Dineen, *J. Appl. Cryst.*, **6**, 474 (1973).
11) A.R. Stokes, *Proc. Phys. Soc. (London)*, **A61**, 382 (1948).
12) S. Ergunn, *J. Appl. Cryst.*, **1**, 19 (1968).
13) A. Kawaguchi, R. Matsui, and K. Katayama, *Bull. Inst. Chem. Res., Kyoto Univ.*, **58**, 470 (1986).
14) 'X-ray Optics' by A.J.C. Wilson, Metheuen, London, 1947.
15) M. Tsuji, A. Uemura, M. Ohara, A. Kawaguchi, K. Katayama, and J. Petermann, *Sen-i Gakkaishi*, **40**, T-580 (1986).